RADIATION RESEARCH 132, 271–276 (1992)

Microdosimetry of Diagnostic X Rays: Applications of the Variance–Covariance Method

J. CHEN,* H. ROOS,† AND A. M. KELLERER*,†

*Institute for Radiation Biology, GSF, Neuherberg, Germany; and †Radiobiological Institute, University of Munich, Germany

CHEN, J., ROOS, H., AND KELLERER, A. M. Microdosimetry of Diagnostic X Rays: Applications of the Variance–Covariance Method. *Radiat. Res.* 132, 271–276 (1992).

Microdosimetric measurements in beams of diagnostic X rays (between 30 and 125 kV) have been performed. In these pulsed radiation fields, microdosimetric measurements are possible only by application of the variance–covariance technique. The dose mean lineal energy, $\bar{y}_D$, is determined for various simulated diameters, at different depths in the absorber, and at different points within the pulse intervals. From the measured temporal dependences one can also obtain values of $\bar{y}_D$ for different X-ray pulse generators. The results demonstrate the potential of the variance–covariance method for a diversity of microdosimetric measurements in radiation protection and in the quality control of radiation beams.

INTRODUCTION

The quality factor in radiation protection is currently defined as a function of the linear energy transfer (L) which can be calculated in radiation fields of known spectral distribution. But the experimental determination of the quality factor, especially for radiation fields with incompletely known spectra, needs to be based on the measurable microdosimetric parameter dose mean lineal energy, $\bar{y}_D$, which is closely related to the dose mean linear energy transfer. This parameter therefore becomes increasingly important in the practice of radiation measurements.

The variance–covariance method permits one to determine $\bar{y}_D$ in time-varying radiation fields (*1*). Until now, several applications of this method have been made. Some experiments were performed in the laboratory with low dose rate (*2, 3*), some were performed with neutron beams (*4, 5*), and some were done with therapeutic electron beams (*6, 7*). All of the experiments show the potential of the variance–covariance method and its applicability in radiation protection and radiation beam control.

However, while microdosimetry in its conventional form has become more and more important in their fields, the variance–covariance method has still not entered into routine practice. We felt, therefore, that a new investigation with added features would be useful.

X rays are widely used in diagnostic radiology, but there are very few microdosimetric measurements so far for such radiation fields. In the pulsed diagnostic radiation fields, the variance method cannot be used, and measurements of single-event spectra would be possible only if one reduced the dose rate sufficiently by increasing the source-to-detector distance, which is usually impracticable. Furthermore, measurements with the single-event technique would require impracticable time for this kind of radiation instrument. With the variance–covariance method one avoids this dilemma. Therefore, a special aim of this paper is to demonstrate the potential of the variance–covariance method in pulsed diagnostic radiation fields. We give new data for these commonly used radiation fields and show that not only the averaged information for a whole pulse train but also the microdosimetric characteristics of individual subpulses can be determined by the variance–covariance method. We achieve this by the use of a sufficiently high sampling frequency.

The measurements with the variance–covariance method were performed in the field of a "two-pulse" X-ray generator for radiography. It will be seen subsequently that measurements on this type of generator provide microdosimetric information even for other pulsed X-ray generators.

MATERIALS AND METHODS

We chose to determine the quality of the diagnostic X rays produced by a Siemens "Nanomobil 2" X-ray generator. It is a two-pulse generator, i.e., there are two sinusoidal pulses within each 20-ms period (see Fig. 1). The anode voltage[1] of this type of instrument can be varied between 30 and 125 kV.

A pair of tissue-equivalent cylindrical proportional counters (height equal to diameter) with methane-based tissue-equivalent gas was employed for the measurements. The geometry and construction of the detectors have been described earlier (*3*). They have tissue-equivalent walls 12 mm thick. The counters are linked to the same gas-flow system and to the same high voltage supply; any fluctuations of gas gain in the two detectors are therefore correlated and can, as is the case with the dose fluctuations, be eliminated with the variance–covariance technique. The proportional counters are calibrated with a collimated ^{241}Am α-particle source for different gas pressures and electrode voltages.

The electronic signal processing system is represented in Fig. 2. Two detectors, A and B, are exposed to the same radiation field and register

[1] The term anode voltage is here used for the maximum of the pulsed potential.

0033-7587/92 $5.00

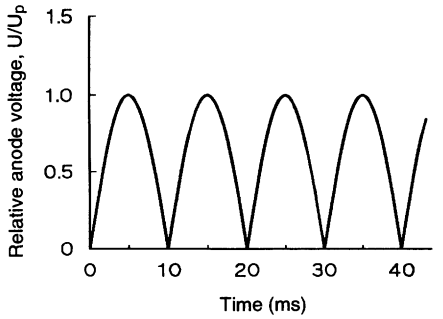

FIG. 1. Pulse form of anode voltage of a two-pulse X-ray generator.

synchronously the electric signals which are proportional to the energy imparted within each of the detectors. The currents from the detectors are measured by electrometers in an integrating mode. The current and the voltage noise of the electrometers are 10^{-15} A and 20 μV (rms), respectively. To achieve optimal resolution, the signals of each irradiation pulse are further amplified to cover most of the dynamic range of the analog-to-digital converter (12-bit). The influences of electronic noise and of the converter's resolution on the measured signals are below 5%.

The digitized data are stored in the computer as time sequences. The variance–covariance method does not require information on the temporal interrelationship of the specific energies registered in consecutive measurement intervals. The information can, however, be used to determine from the data for the two-pulse generator the dose mean lineal energy as a function of instantaneous voltage, and thus the variations of $\bar{y}_D$ within irradiation pulses. Figure 3 shows, as an example, the measured data from three irradiation pulses for two detectors; the duration of the sampling intervals was 100 μs. Due to attenuation of the softer X rays as well as the decline of photon yield at low anode voltages, Fig. 3 shows "zero" energy imparted during an appreciable portion of each cycle.

From paired data for the two detectors the mean, $\bar{\epsilon}$, of the energy imparted, its relative variance, V, and its relative covariance, C, are determined. The dose mean of the energy imparted per energy deposition event is given by the variance–covariance method.

$$\bar{\epsilon}_D = (V - C) \cdot \bar{\epsilon}$$

The corresponding values of the dose mean lineal energy, $\bar{y}_D$, are given by

$$\bar{y}_D = \bar{\epsilon}_D / \bar{l},$$

where $\bar{l}$ is the mean chord length of the simulated volume.

Figure 3 indicates that detector B registered a somewhat higher dose rate than detector A. However, the values of the microdosimetric parameters,

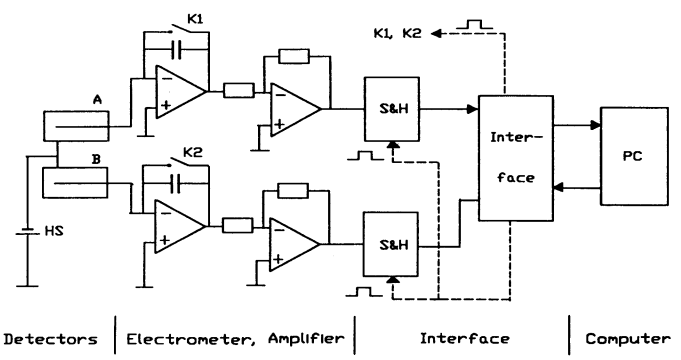

FIG. 2. Electronic signal processing system to perform measurements with the variance–covariance technique.

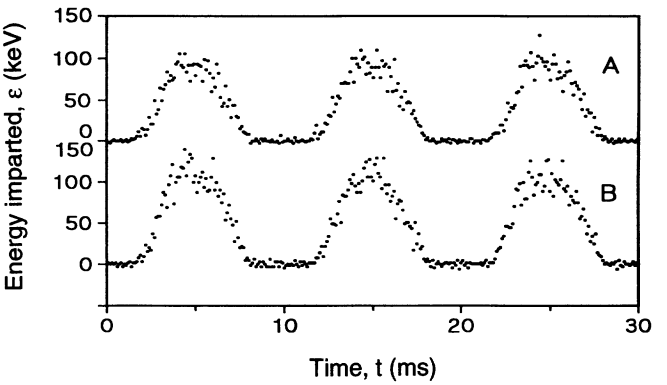

FIG. 3. Data for the energy imparted in sampling intervals of 100 μs from the pair of detectors. The peak voltage on the anode is 90 kV; the simulated diameter of the cylindrical detector volume is 0.5 μm.

as well as those of the relative variance and the relative covariance, are not dependent on dose rate, and equality of the dose rate in the two detectors or centering of two detectors in radiation field is therefore not a requirement of the variance–covariance method.

Another advantage of the method is the correction for correlated additive disturbances (*3, 4, 7*), such as pick-up, that affect the two detectors equally. As shown in the Appendix, such disturbances are eliminated if the parameters for the two detectors are averaged.

$$\bar{y}_D = (\bar{y}_{D,A} + \bar{y}_{D,B})/2$$

$\bar{y}_D$ FOR VARIOUS SITE SIZES AND DIFFERENT ANODE VOLTAGES

The dose mean lineal energies, $\bar{y}_D$, for simulated diameters of 0.2, 0.5, 1, and 8 μm were measured at different anode voltages between 30 or 35 and 125 kV (Table I). For simulated diameters smaller than 1 μm signals at 30 kV were too weak to be measured with the required accuracy. All measurements were performed with a filter equivalent to 2 mm of aluminum. Figure 4 and Table I summarize the results. The standard deviations given in Fig. 4 are devia-

TABLE I
The Dose Mean Lineal Energy (keV/μm) at Different Anode Voltages (kV) for Two-Pulse X-Ray Generator

Voltage	0.2 μm	0.5 μm	1 μm	8 μm
30			3.42 ± 0.25	1.98 ± 0.03
35	5.89 ± 0.60	4.55 ± 0.24	3.35 ± 0.11	2.17 ± 0.12
42				1.84 ± 0.07
48	5.37 ± 0.54	4.30 ± 0.28	3.21 ± 0.09	
51				1.50 ± 0.02
60	5.98 ± 0.48	4.27 ± 0.25	3.19 ± 0.16	1.41 ± 0.06
75	5.82 ± 0.48	4.38 ± 0.13	2.94 ± 0.05	1.46 ± 0.06
90	5.86 ± 0.10	4.36 ± 0.19	2.97 ± 0.03	1.47 ± 0.08
110	6.10 ± 0.62	4.37 ± 0.27	2.94 ± 0.04	1.47 ± 0.09
125	5.93 ± 0.44	4.38 ± 0.35	2.99 ± 0.04	1.35 ± 0.04

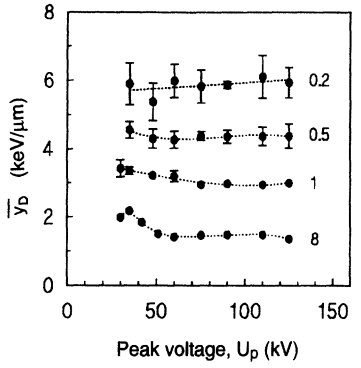

FIG. 4. Dose mean lineal energy as function of the peak voltage at different simulated diameters. The bars represent the standard deviations between different measurements. At large simulated diameters (1 and 8 μm) most error bars are too small to be drawn.

tions between different measurements; they depend not only on electronic noise of the measurement system but also on the noise of the radiation generator and of the environment.

Dependence on Site Size

As seen in Fig. 4, the dose mean lineal energy increases as the simulated diameter decreases. This is shown more directly in Fig. 5, which gives the overall values of $\bar{y}_D$ for the entire pulse distribution as a function of diameter. The values for the points are averages over the range of possible voltages; they are plotted together with their standard deviations, which are small.

The decrease in $\bar{y}_D$ with increasing site size is a general feature of microdosimetric distributions. At large site sizes and with short particle ranges, it reflects the increasing fraction of "starters" and "stoppers" and then of "insiders," i.e., of particles that do not traverse the entire site. In the present case one deals with electrons that have, on average, ranges that are considerably larger than the site sizes that are investigated. But even under this condition $\bar{y}_D$ decreases with increasing site diameter, because there are only small distances over which the electrons exhibit high LET; i.e., the small range of the track ends accounts for the large values of y in small sites.

A further very important factor at small site sizes is energy loss straggling, i.e., the clustering of energy in δ rays or groups of δ rays. Such local energy concentrations can lead to high values of $\bar{y}_D$ in small regions, but less so in larger sites.

The joint influence of the different, complex factors on $\bar{y}_D$ is more clearly seen in the fundamental relationship that links $\bar{y}_D$ to the proximity function, $t(x)$, of a radiation.

$$\bar{y}_D = \frac{1}{\bar{l}} \int_0^d U(x/d) \cdot t(x) \cdot dx$$

The proximity function, $t(x)$, is defined as the distribution of distances between all energy transfers in particle tracks, and $U(x/d)$ is the geometric reduction factor of a given site, i.e., the sum distribution of chord lengths of the site for so-called internal source randomness (*8*). The diameter of the site is d. For a sphere or a right cylinder (cylinder length equals the diameter of the cylinder) the mean chord length is

$$\bar{l} = 2d/3.$$

Using the distance scaled by the diameter, $x' = x/d$, one has

$$\bar{y}_D = \frac{3}{2} \int_0^1 U(x') \cdot t(d \cdot x') \cdot dx'.$$

Apart from its behavior at very small distance $t(x)$ is a monotonously decreasing function of distance x, and the formula shows that $\bar{y}_D$ must be a monotonously decreasing function of d. The argument applies to any function $U(x)$, i.e., to an arbitrary convex shape.

Dependence on Anode Voltage

The dependence of $\bar{y}_D$ on anode voltage is far more complex. It reflects the change of electron energies with photon energies, and the change in $\bar{y}_D$ with changing electron energy at specified site sizes. Both dependences are nonmonotonic. For the anode voltages in the range of 30 to 125 kV and for the filter and the detector wall thickness that are employed in the present experiments the average photon energies vary from about 25 to 60 keV (*9*). Due to the variation of relative cross sections for the photo- and Compton effects in this range of photon energies, the average initial energy of the released electrons decreases with increasing photon energy, as seen in Fig. 6. There is then an increase in the average LET. However, $\bar{y}_D$ increases only at small site sizes, while there is a decrease with decreasing electron energy at larger site sizes. Figure 4 shows all these complexities.

Due to the thickness of the filter and of the detector wall the spectra of X rays in the detector volume are very narrow for anode voltages around 35 kV, i.e., they are almost mono-

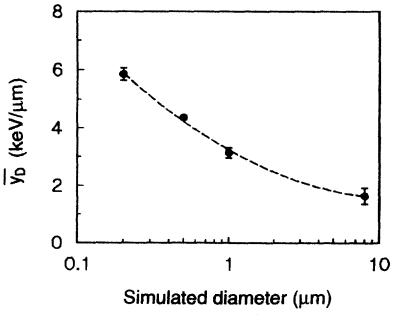

FIG. 5. The dose mean lineal energy as function of the site diameter.

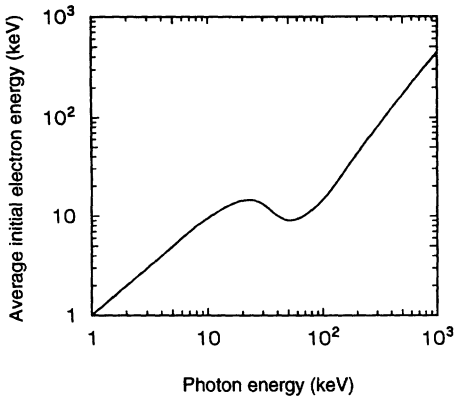

FIG. 6. Average initial energy of the (first collision) released electrons as a function of photon energy in water.

energetic. The values of $\bar{y}_D$ for these anode voltages agree well with the data for monoenergetic photons obtained by Kliauga and Dvorak (*10*) in single-event measurements.

$\bar{y}_D$ AT DIFFERENT DEPTHS

Measurements of absorbed dose as a function of depth in a receptor are fundamental to dosimetry. But beyond the dose distributions one needs to consider also the variation of radiation quality with depth. It is therefore of interest to examine the dependence of the lineal energy on depth.

Different depths in tissue were simulated simply by placing different acrylic blocks (density 1.17 g/cm^3) in front of detectors. The thickness of the blocks was changed from 0 to 11.5 cm. Taking the detector wall (A150, density 1.12 g/cm^3) into account, one simulates in this way depths in tissue from 1.34 to 14.8 cm. There appeared to be no need for providing backscatter beyond that taking place in the detector wall. The measurements were performed for anode voltages of 42 and 70 kV, and with a filter equivalent to 1 mm of aluminum. The results are given in Fig. 7.

For a small simulated site the dose mean lineal energy decreases somewhat with increased depth, as seen in Fig. 7. This dependence is in line with the "hardening" of the radiation quality that has been demonstrated by Hahn[2] in Monte Carlo calculations for photon energies below 100 keV.

VARIATION OF THE LINEAL ENERGY WITH PULSE PHASE

Using the temporal information in the measured data, one can determine the dose mean lineal energy for any point within the radiation pulse; one merely needs to select in the analysis the observations at this point. As examples, two such phase dependences are shown in Fig. 8.

[2] K. Hahn and A. M. Kellerer, private communication, 1990.

For a simulated diameter of 1 μm and an anode voltage of 75 kV, the dose mean lineal energy does not vary substantially. This agrees with the results for 1 μm in Fig. 4, which show little change in $\bar{y}_D$ with anode voltage. In contrast, one sees in Fig. 4 a significant rise in the dose mean lineal energy with anode voltages below 50 kV and at a simulated diameter of 8 μm. The anode potential is pulsed, as illustrated in Fig. 1, and the dose mean lineal energy varies in phase with the anode potential. The variations in $\bar{y}_D$ are exemplified in Fig. 8 for a simulated diameter of 8 μm and for the anode voltage 51 kV; the maximal difference in $\bar{y}_D$ is, in this case, about 44%.

These two examples demonstrate the potential and the diverse possibilities of the variance–covariance technique for the measurement, with high sampling frequency, of the time dependence of microdosimetric parameters in periodic radiation fields.

$\bar{y}_D$ FOR DIFFERENT X-RAY GENERATORS

A 2-pulse generator exhibits variations of the anode voltage that are larger than those for 6-pulse or 12-pulse generators. Using part of the data on the voltage dependence for a 2-pulse generator one can therefore deduce the variations for 6-pulse or 12-pulse generators. As it happens, the superposition pulses for 6- or 12-pulse generators are of the same shape as subregions around the peaks of the 2-pulse generator (see Fig. 9). It is therefore particularly easy to derive the values $\bar{y}_D$ for the multipulse generators by using only the suitably restricted pulse data measured for the 2-pulse generator.

Results are given in Fig. 10. The decrease in $\bar{y}_D$ with anode voltage for generators of different pulse numbers is represented. More marked dependences of $\bar{y}_D$ would have to be seen, if the measurements were performed with detectors of thin wall or with wall-less counters; the role of low-energy photons would then be more important.

CONCLUSION

The measured microdosimetric data for the commonly used diagnostic X rays show the considerable potential of

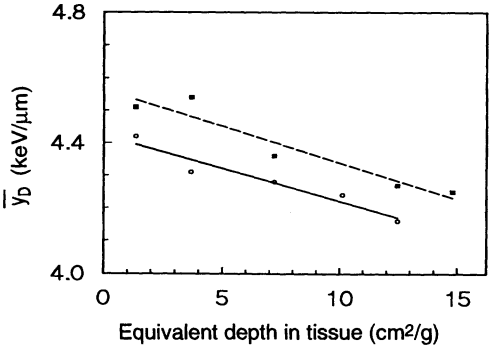

FIG. 7. Depth dependence of the dose mean lineal energy for anode voltages of (—) 42 and (– –) 70 kV. The simulated diameter is 0.5 μm.

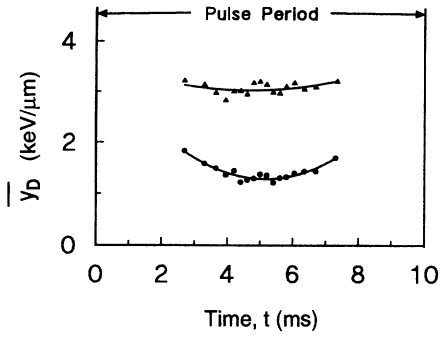

FIG. 8. Variation of the dose mean lineal energy with the pulse phase of the periodic X-ray fields. (△) 1 μm, 75 kV; (●) 8 μm, 51 kV.

the variance–covariance method. Such data could not readily be obtained with the conventional single-event technique in microdosimetry, and they would, of course, be impossible with the simple variance technique. The variance–covariance method is thus seen to be a useful technique for radiation protection and quality control, especially in time-varying or in incompletely known radiation fields.

APPENDIX

Reduction of the Influence of Correlated Additive Noise by Averaging of the Parameters for the Two Detectors

The signal to be measured, u_s, is accompanied by the noise, u_N. The result of a measurement is then

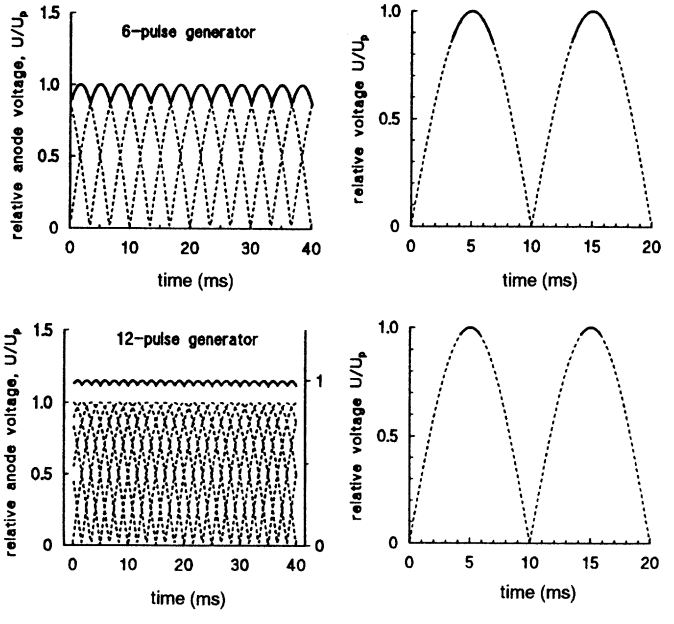

FIG. 9. Pulse form of anode voltage of a 6-pulse and a 12-pulse X-ray generator. The pulse forms of the 6-pulse and 12-pulse generators are part of that performed by the 2-pulse generator.

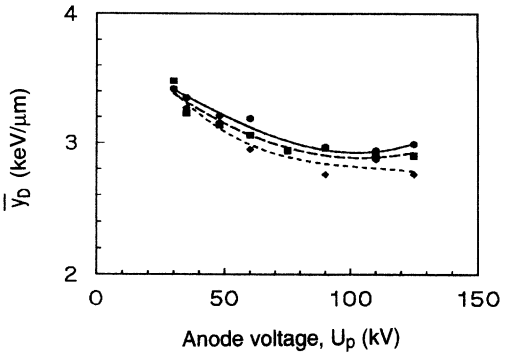

FIG. 10. Dose mean lineal energy as function of anode voltage for the (●) 2-pulse, (■) 6-pulse, and (♦) 12-pulse generator. The simulated diameter is 1 μm.

$$u_m = u_s + u_N.$$

The mean value $\bar{u}_m$, the variance V_m and the covariance C_m are given by the relationships

$$\overline{u_m} = \overline{u_s}$$

$$V_m = V_s + V_N$$

$$C_m = C_s + C_N.$$

According to the variance–covariance method one derives from detector A the dose mean value

$$\bar{u}_{s,D} = \frac{V_s(A)}{\bar{u}_s(A)} - \frac{C_s}{\bar{u}_s(B)}.$$

But because of the noise, u_N, one obtains

$$\bar{u}_{m,D}(A) = \frac{V_m(A)}{\bar{u}_m(A)} - \frac{C_m}{\bar{u}_m(B)} = \bar{u}_{s,D} + \frac{V_N(A)}{\bar{u}_s(A)} - \frac{C_N}{\bar{u}_s(B)}.$$

Similarly, one obtains from detector B

$$\bar{u}_{m,D}(B) = \frac{V_m(B)}{\bar{u}_m(B)} - \frac{C_m}{\bar{u}_m(A)} = \bar{u}_{s,D} + \frac{V_N(B)}{\bar{u}_s(B)} - \frac{C_N}{\bar{u}_s(A)}.$$

For correlated noise one has

$$V_N(A) = V_N(B) = C_N = \sigma^2.$$

The average of the two dose mean values from detectors A and B equals

$$\frac{\bar{u}_{m,D}(A) + \bar{u}_{m,D}(B)}{2} = \bar{u}_{s,D}$$

$$+ \frac{\sigma^2}{2}\left(\frac{1}{\bar{u}_s(A)} - \frac{1}{\bar{u}_s(B)} + \frac{1}{\bar{u}_s(B)} - \frac{1}{\bar{u}_s(A)}\right) = \bar{u}_{s,D}.$$

Thus the correlated additive noise has no influence on the results of the variance–covariance method, if the averaging is performed.

ACKNOWLEDGMENTS

This work was supported by EURATOM Contract B17-0025-C. We are grateful to Prof. Harald H. Rossi for helpful discussions.

RECEIVED: December 20, 1991; ACCEPTED: June 8, 1992

REFERENCES

1. A. M. Kellerer and H. H. Rossi, On the determination of microdosimetric parameters in time-varying radiation fields: The variance–covariance method. *Radiat. Res.* **97,** 237–245 (1984).
2. J. Breckow, A. Wenning, H. Roos, and A. M. Kellerer, The variance–covariance method: Microdosimetry in time-varying low dose-rate radiation fields. *Radiat. Environ. Biophys.* **27,** 247–259 (1988).
3. J. Chen, J. Breckow, H. Roos, and A. M. Kellerer, Further development of the variance–covariance method. *Radiat. Prot. Dosim.* **31,** 171–174 (1990).
4. L. Lindborg, P. Kliauga, S. Marino, and H. H. Rossi, Variance–covariance measurements of dose mean lineal energy in a neutron beam. *Radiat. Prot. Dosim.* **13,** 347–351 (1985).
5. P. Goldhagen, G. Randers-Pehrson, S. A. Marino, and P. Kliauga, *Variance–covariance* measurements of y_D for 15 MeV neutrons in a wide range of site sizes. *Radiat. Prot. Dosim.* **31,** 167–170 (1990).
6. P. Kliauga, H. Amols, and L. Lindborg, Microdosimetry of pulsed radiation fields employing the variance–covariance method. *Radiat. Res.* **105,** 129–137 (1986).
7. H. B. Honoré, K. A. Jessen, and H. H. Nielsen, Variance–covariance measurements of the dose mean lineal energy in beams for radiotherapy. *Radiat. Prot. Dosim.* **31,** 453–455 (1990).
8. A. M. Kellerer and D. Chmelevsky, Concepts of microdosimetry, III. Mean values of the microdosimetric distributions. *Radiat. Environ. Biophys.* **12,** 321–335 (1975).
9. W. W. Seelentag, W. Panzer, G. Drexler, L. Platz, and F. Santner, *A Catalogue of Spectra for the Calibration of Dosemeters.* GSF Bericht 560, 1979.
10. P. Kliauga and R. Dvorak, Microdosimetric measurements of ionization by monoenergetic photons. *Radiat. Res.* **73,** 1–20 (1978).